

Research Paper

Coumarin formation in novobiocin biosynthesis: β -hydroxylation of the aminoacyl enzyme tyrosyl-*S*-NovH by a cytochrome P450 NovI

Huawei Chen, Christopher T. Walsh*

Department of Biological Chemistry and Molecular Pharmacology, Harvard Medical School, 240 Longwood Avenue, Boston, MA 02115, USA

Received 24 November 2000; revisions requested 24 January 2001; revisions received 5 February 2001; accepted 6 February 2001

First published online 22 February 2001

Abstract

Background: Coumarin group antibiotics, such as novobiocin, coumermycin A₁ and clorobiocin, are potent inhibitors of DNA gyrase. These antibiotics have been isolated from various *Streptomyces* species and all possess a 3-amino-4-hydroxy-coumarin moiety as their structural core. Prior labeling experiments on novobiocin established that the coumarin moiety was derived from L-tyrosine, probably via a β -hydroxy-tyrosine (β -OH-Tyr) intermediate. Recently the novobiocin gene cluster from *Streptomyces spheroides* was cloned and sequenced and allows analysis of the biosynthesis of the coumarin at the biochemical level using overexpressed and purified proteins.

Results: Two open reading frames (ORFs), NovH and NovI, from the novobiocin producer *S. spheroides* have been over-expressed in *Escherichia coli*, purified and characterized for tyrosine activation and oxygenation which are the initial steps in coumarin formation. The 65 kDa NovH has two predicted domains, an adenylation (A) and a peptidyl carrier protein (PCP), reminiscent of non-ribosomal peptide synthetases. Purified NovH catalyzes L-tyrosyl-AMP formation by its A domain, can be posttranslationally phosphopantetheinylated on the PCP domain, and accumulates the covalent L-tyrosyl-*S*-enzyme intermediate on the holo PCP domain. The second enzyme in the pathway, NovI, is a 45 kDa heme protein that functions as a cytochrome P450-

type monooxygenase with specificity for the tyrosyl-*S*-NovH acyl enzyme. The product β -OH-tyrosyl-*S*-NovH was detected by alkaline release and high performance liquid chromatography analysis of radioactive [³H] β -OH-Tyr and by mass spectrometry. Also detected was 4-OH-benzaldehyde, a retro aldol breakdown product of β -OH-Tyr. The amino acid released was (3*R*,2*S*)-3-OH-Tyr by comparison with authentic standards.

Conclusions: This work establishes that NovH and NovI are responsible for the formation of a β -OH-Tyr intermediate that is covalently tethered to NovH in novobiocin biosynthesis. Comparable A-PCP/P450 pairs for amino acid β -hydroxylation are found in various biosynthetic gene clusters, such as ORF19/ORF20 in the chloroeremomycin cluster for tyrosine, CumC/CumD in the coumermycin A₁ cluster for tyrosine, and NikP1/NikQ in the nikkomycin cluster for histidine. This phenomenon of covalent docking of the amino acid in a kinetically stable thioester linkage prior to chemical modification by downstream tailoring enzymes, could represent a common strategy for controlling the partitioning of the amino acid for incorporation into secondary metabolites. © 2001 Elsevier Science Ltd. All rights reserved.

Keywords: Novobiocin; Coumarin; β -Hydroxy-tyrosine; Cytochrome P450 monooxygenase; Non-ribosomal peptide synthetase

1. Introduction

The coumarin group of antibiotics, such as novobiocin, clorobiocin and coumermycin A₁ (Fig. 1A), are secondary metabolites from certain *Streptomyces* species and exert

their antibacterial activity by inhibition of the type II DNA topoisomerase DNA gyrase [1–4]. These inhibitors have a 3-amino-4-hydroxy-coumarin and a substituted deoxysugar noviose as a common core that is essential for their biological activity. Clorobiocin differs from novobiocin in that the methyl group at the C-8 of coumarin ring is replaced by a chlorine atom, and the carbamoyl at the C-3' of the noviose is substituted by a 5-methyl-2-pyrrolcarboxyl group. Coumermycin A₁ contains two of the coumarin–noviose core joined by a 3-methyl-2,4-dicarboxyl pyrrole linker and has the same substituted noviose as in clorobiocin. Gyrase inhibitors, including the structurally similar quinolones [5], block DNA replication, induce

Abbreviations: A, adenylation domain; β -OH-Tyr, β -hydroxy-tyrosine; MALDI-TOF, matrix-assisted laser desorption ionization time-of-flight; PCP, peptidyl carrier protein; NRPS, non-ribosomal peptide synthetase; rt, retention time

* Correspondence: Christopher T. Walsh;
E-mail: christopher_walsh@hms.harvard.edu

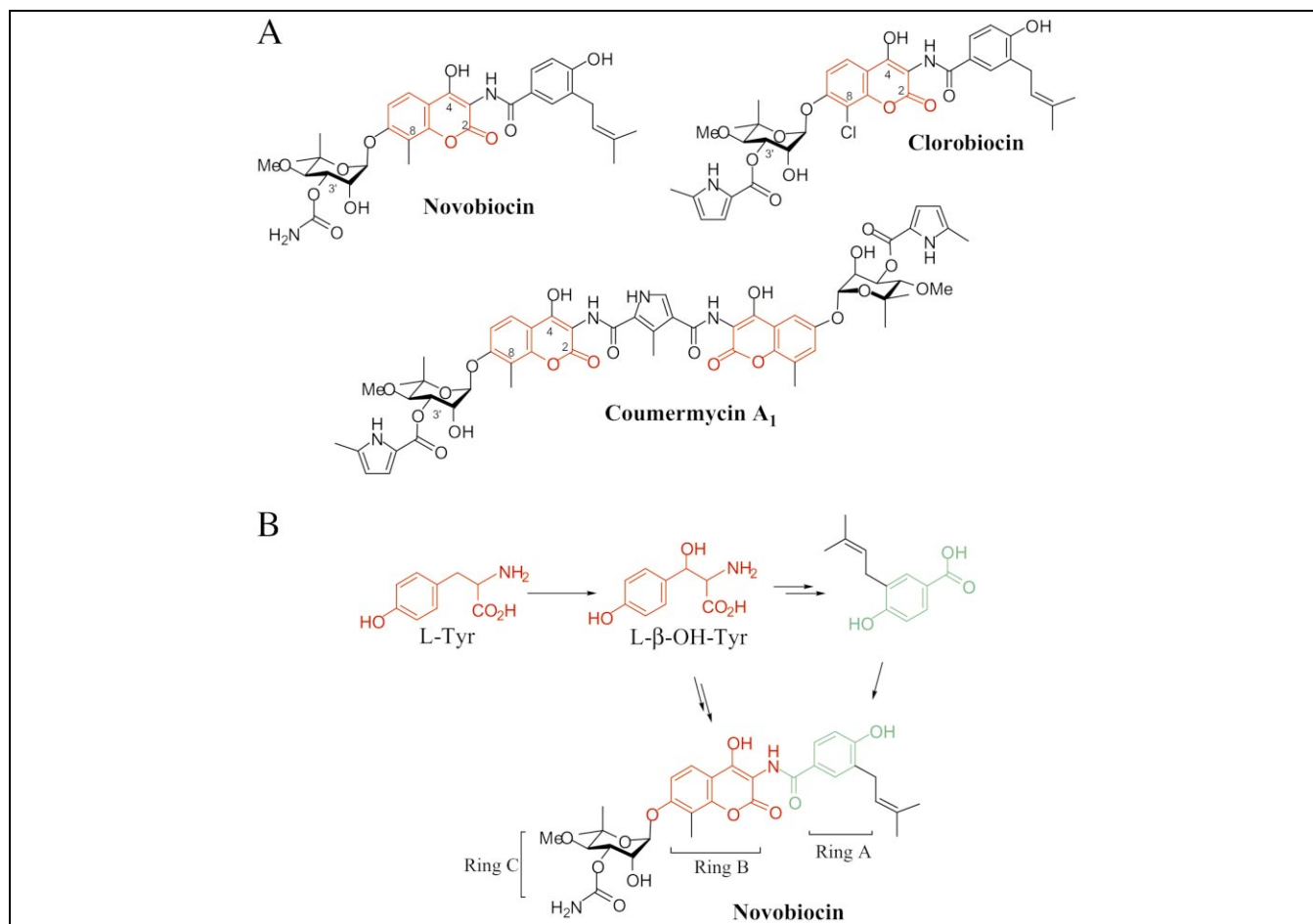


Fig. 1. (A) Chemical structures of coumarin group antibiotics isolated from *Streptomyces*. The coumarin moiety in the natural products is highlighted in red. (B) The substituted coumarin (ring B, red) and the 4-OH benzoyl moiety (ring A, aqua) in novobiocin were derived from L-Tyr based on earlier labeling studies. β -OH-Tyr is proposed to be a common intermediate in these two biosynthetic pathways.

SOS repair systems and eventually cause bacterial cell death. Previous kinetic and structural studies [3,4,6,7] have shown that coumarin group antibiotics are competitive inhibitors of ATP binding to the gyrase B subunit. Substitution of a 3'-noviose carbamoyl (novobiocin) for a 5-methyl-2-pyrrolicarboxyl group (clorobiocin) results in an enhanced inhibitory activity toward gyrase in vitro [8]. Coumermycin A₁, on the other hand, acting like a novobiocin dimer, stabilizes a dimer form of the 43 kDa fragment of GyrB [9]. Early labeling studies have established that the substituted coumarin and the prenylated benzoic acid moieties were derived from L-Tyr while the noviose was from glucose [10–12]. Recently, insights into the biosynthesis of novobiocin were obtained by the sequencing of the *nov* gene cluster from *Streptomyces spheroides* [13]. As shown in Fig. 1B, it is possible that β -hydroxy-tyrosine (β -OH-Tyr) could be a common precursor of both substituted coumarin and benzoyl moieties. An amide synthase responsible for joining these two moieties has been purified and characterized very recently [14].

The defined *nov* genes in the novobiocin cluster [13] provide a chance to elucidate some key steps for novobiocin assembly in vitro. We focused on delineating the enzymes that create the coumarin ring scaffold. In this work we have investigated two adjacent open reading frames (ORFs) in the *nov* cluster, NovH and NovI, to establish their role in tyrosine activation and modification in the coumarin-forming pathway. Sequence homology analysis suggested NovH is related to amino acid activating modules of non-ribosomal peptide synthetases (NRPSs) in having two predicted domains, an amino acid adenylating (A) domain and an aminoacyl-tethering peptidyl carrier protein (PCP) domain [15–17]. The second protein, NovI, has similarities to subclasses of cytochrome P450 monooxygenases [13,18–20]. Here we report that NovH activates L-Tyr and forms a tyrosyl-S-NovH acyl-S-enzyme that is the substrate for regio and stereospecific hydroxylation by NovI to yield a β -OH-tyrosyl group still tethered on the NovH PCP domain.

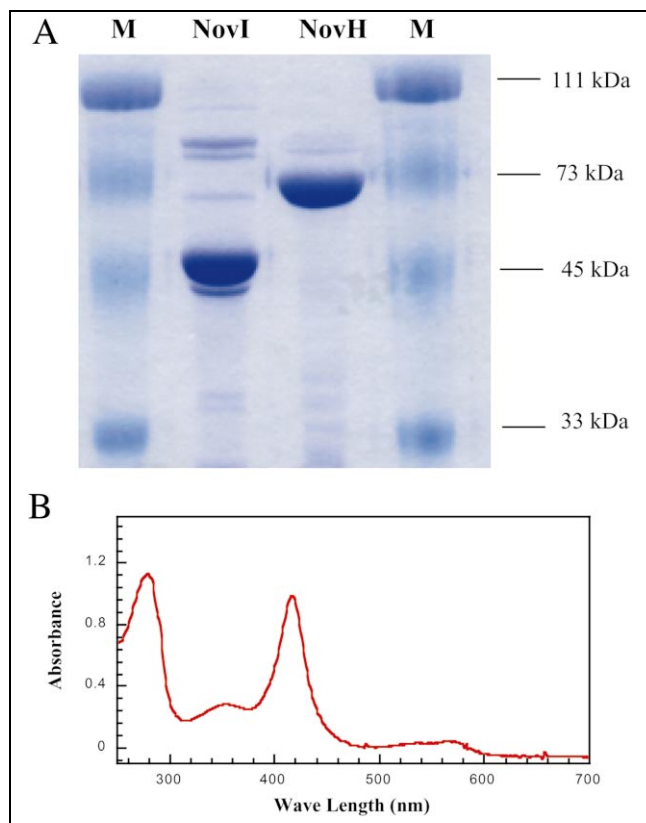


Fig. 2. (A) Coomassie brilliant blue-stained 10% SDS-PAGE gel showing NovH and NovI proteins purified by nickel chelate chromatography. Lanes 1 and 4, molecular weight standards; lane 2, purified NovI; lane 3, purified NovH. (B) UV-visible spectrum of the purified NovI protein. The NovI protein was isolated as a holo protein containing 1 equivalent of heme cofactor based on the calculation with the extinction coefficient (ϵ) for NovI protein and the heme cofactor of 0.061 and $0.055 \mu\text{M}^{-1} \text{cm}^{-1}$ at λ_{max} 279 and 416 nm, respectively.

2. Results

2.1. Expression and purification of *S. spheroides* NovH and NovI in *Escherichia coli*

Two enzymes that may be responsible for the initial steps in the biogenesis of the coumarin ring in novobiocin were expressed and purified. NovH is a didomain NRPS with a putative *L*-tyrosine specific A domain and a C-terminal PCP domain while NovI shows significant sequence homology to cytochrome P450 hydroxylases. *E. coli* BL21(DE3) cells harboring NovH expression constructs grown at temperatures above 30°C after induction yielded only insoluble protein. To obtain soluble protein, cells were cooled to 24°C before induction with $50 \mu\text{M}$ of isopropyl β -D-thiogalactopyranoside (IPTG). A C-terminal His6-tagged NovH was purified by nickel affinity chromatography in apo-form with a protein yield of 30 mg/l . NovI was expressed as inclusion bodies when grown above 20°C , but soluble protein was obtained by growing at 15°C for 72 h without IPTG induction. NovI was purified as an N-terminal His10-tagged fusion protein by nickel chelate chromatography with a protein yield of 5 mg/l of culture. Both proteins were purified to near homogeneity with a correct molecular weight as judged by SDS-PAGE (Fig. 2A). As shown in Fig. 2B, the UV-visible spectrum of the purified NovI indicates that NovI was fully loaded with the heme cofactor.

2.2. Characterization of NovH as a *L*-Tyr specific didomain NRPS to generate a *L*-tyrosyl-S-NovH intermediate

2.2.1. Posttranslational modification of PCP domain with a PPTase

Protein sequence alignment indicated that the C-terminal portion of NovH resembles a typical PCP domain in NRPS systems with a conserved active site Ser561 sur-

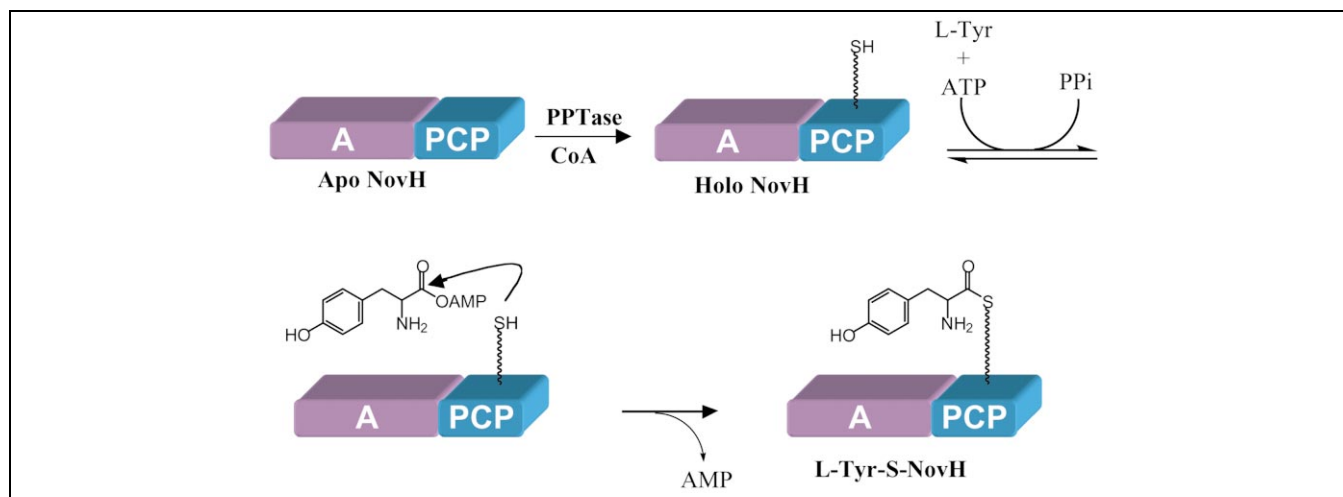


Fig. 3. Schematic representation of the proposed functions of NovH. NovH isolated from *E. coli* needs to be primed by a PPTase with CoA to become a holo-protein by installing a prosthetic P-pant group at the active site Ser561 on the PCP domain [13]. The A domain activates *L*-Tyr as *L*-tyrosyl-AMP and then transfers the *L*-tyrosyl group to the HS-pant-PCP domain of NovH through thioester formation.

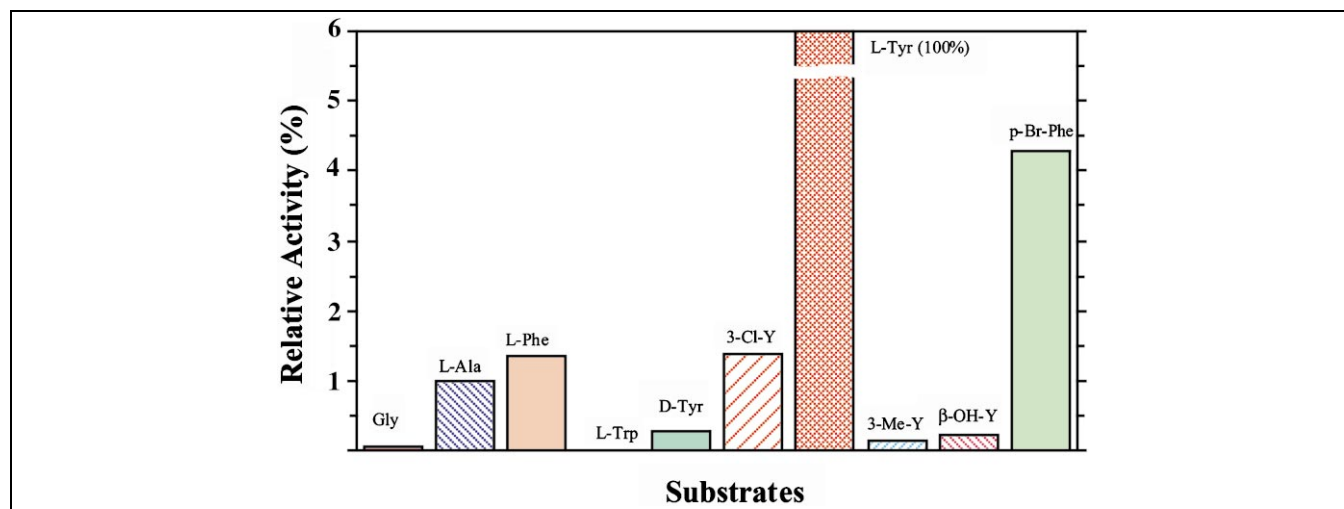


Fig. 4. Relative activity of several amino acids towards the A domain of NovH as assessed by ATP- 32 Pi exchange assays. L-phenyl-Gly, L-*p*-OH-phenyl-Gly, *p*-OH-phenyl-acetate, and *p*-OH-phenyl-pyruvate were also examined and all of them failed to show any detectable activity (data not shown).

rounded by a canonical sequence (549 DVRSNFFE-MGGNSILAVDL 567) for posttranslational priming [13]. Purified NovH protein was assayed for covalent attachment of a phosphopantetheinyl (P-pant) group by Sfp [21], a phosphopantetheinyltransferase (PPTase) from surfactin synthetase from *Bacillus subtilis* (Fig. 3). Under the assay conditions, Sfp rapidly (<3 min) modified the NovH with 3 H]CoA as substrate (data not shown) [21,22]. The percentage of P-pant incorporation was estimated to be $>95\%$ based on the specific radioactivity of 3 H]CoA and the concentration of NovH. Thus, NovH was purified as an apo protein from *E. coli*, typical for other heterologously expressed NRPS PCP domains [23], but could be converted fully to the holo-PCP form by Sfp in vitro.

2.2.2. A domain selectivity of NovH

The A domain of an NRPS is expected to be bifunctional, i.e. activation of the amino acid substrate and subsequent ligation of aminoacyl-AMP to the downstream holo-PCP domain, as depicted in Fig. 3. The activity of the NovH A domain, aminoacyl adenylate formation, was assayed by a substrate-dependent ATP- 32 Pi exchange reaction. The relative activities of the amino acid substrates tested are displayed in Fig. 4. The NovH A domain was selective for both the chirality of α -carbon and properties of the side chain group. Only L-Tyr served as a competent substrate for the NovH A domain. While D-Tyr, Gly, L-Trp, 3-methyl-L-Tyr, and (2*S*,3*R*)- β -OH-Tyr were essentially inactive, L-Ala, L-Phe, 3-chloro-L-Tyr, and *p*-bromo-DL-Phe had marginal activities with an apparent k_{obs} of 1.0–4.5% relative to L-Tyr (Fig. 4). The kinetic parameters of the ATP-Pi exchange assays of several amino acids are summarized in Table 1. Overall the $k_{\text{cat}}/K_{\text{m}}$ values agree well with the k_{obs} measurements

shown in Fig. 4 with L-Tyr showing the highest activity with a k_{cat} and K_{m} value of 15 min^{-1} and 1.4 mM , respectively. Compounds *p*-bromo-DL-Phe and L-Phe possessed a slightly smaller K_{m} , but showed a dramatic reduced k_{cat} value, indicating the importance of the *para*-OH group of L-Tyr for catalysis. Substitution on the *meta* position had an adversary effect for both k_{cat} and K_{m} and the bulkier methyl group rendered 3-Me-L-Tyr a much worse substrate than 3-Cl-L-Tyr.

2.2.3. Auto-aminoacylation of NovH with 3 H]Tyr

The above ATP-Pi exchange assay established that the A domain of NovH can selectively activate L-Tyr as Tyr-AMP. The ability of holo-NovH to ligate the activated L-Tyr onto the thiol of the P-pant arm on the PCP domain was assayed using 3 H]L-Tyr as substrate. As shown in Fig. 5A,B, SDS-PAGE and autoradiographic analysis indicated ATP-dependent covalent loading of L-Tyr onto NovH. Without pretreatment of NovH with Sfp, no ligation of L-Tyr to NovH was observed, implying that L-Tyr labeling was specific to the PCP domain, and further re-

Table 1

Kinetic parameters of the ATP- 32 Pi assays of NovH A domain

Substrate	k_{cat} (min^{-1})	K_{m} (mM)	$k_{\text{cat}}/K_{\text{m}}$	Selectivity
L-Tyr	15.0 ± 0.3	1.39 ± 0.05	10.8	100
<i>p</i> -Br-DL-Phe	0.44 ± 0.03	0.84 ± 0.14	0.52	4.8
L-Phe	0.13 ± 0.01	0.89 ± 0.19	0.15	1.4
3-Cl-L-Tyr	0.23 ± 0.03	2.17 ± 0.34	0.11	1.0
3-Me-L-Tyr	0.083 ± 0.009	6.13 ± 0.74	0.014	0.13

Reactions for L-Tyr were carried out with $4 \mu\text{M}$ of NovH and terminated after 8 min incubation at 24°C . For incubations of L-Phe, *p*-bromo-DL-Phe (*p*-Br-DL-Phe), 3-chloro-L-Tyr (3-Cl-L-Tyr), and 3-methyl-L-Tyr (3-Me-L-Tyr), $12 \mu\text{M}$ of NovH was used and the reactions were allowed to continue for 23 min at 24°C . See Section 5 for details.

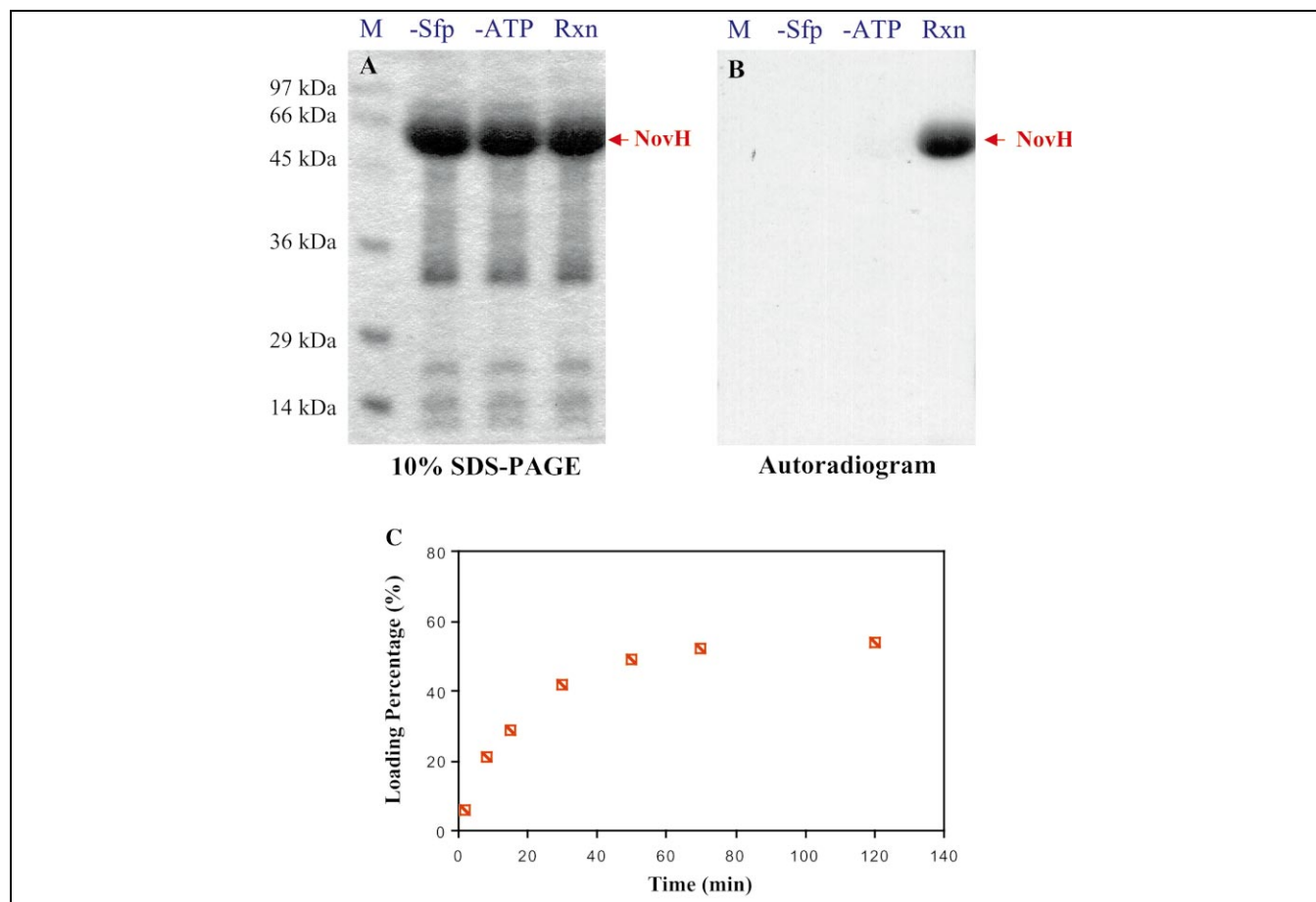


Fig. 5. Demonstration of self aminoacylation of NovH with [^3H]L-Tyr depending on Sfp treatment and ATP. (A) Coomassie brilliant blue-stained 10% SDS-PAGE gel of various reaction mixtures. Lane 1, molecular weight markers; lane 2, control reaction without Sfp treatment; lane 3, control reaction without adding ATP; lane 4, complete reaction. (B) Autoradiogram of this gel. (C) Time course of [^3H]L-Tyr aminoacylation of holo NovH self-catalyzed by the A domain. Radiolabeled substrate incorporation was measured by TCA precipitation of the proteins followed by liquid scintillation counting. See Section 5 for detailed information.

inforcing the evidence that NovH was purified in the apo-protein form. A time course of NovH covalent auto-aminoacylation is shown in Fig. 5C. Under the conditions used for the assays, self-aminoacylation was a rather slow process and it took ~ 50 min to plateau at a final stoichiometry of 0.55 equivalent of L-Tyr-S-NovH.

2.3. Characterization of NovI as a cytochrome P450 monooxygenase that hydroxylates L-tyrosyl-S-NovH in a regio- and stereospecific manner

2.3.1. Incubation of NovI with [^3H]L-tyrosyl-S-NovH

As shown in Fig. 6, NovI was anticipated to function as

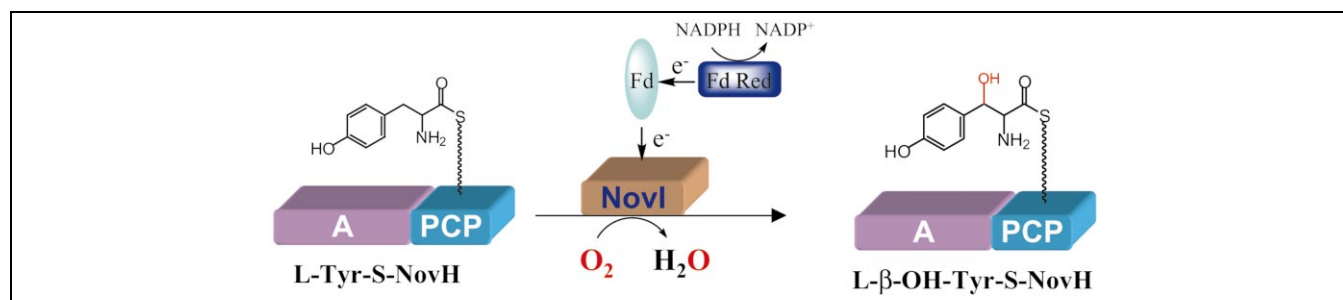


Fig. 6. Schematic representation of the reaction effected by the cytochrome P450 monooxygenase NovI. The putative substrates are L-tyrosyl-S-NovH and molecular oxygen. While the substrate L-tyrosyl-S-NovH provides two electrons for a single round of the hydroxylation reaction, the other two electrons needed to reduce the oxygen atom are provided by NADPH via two-electron transfer effected by electron transfer proteins ferredoxin (Fd) and ferredoxin reductase (Fd Red). The electron transfer route is from NADPH \rightarrow FAD in Fd Red \rightarrow Fe-S center in Fd \rightarrow Heme in NovI \rightarrow oxygen. Heterologous electron transfer proteins from spinach were used in this study because the *S. spheroides* electron transfer proteins for NovI have not yet been identified.

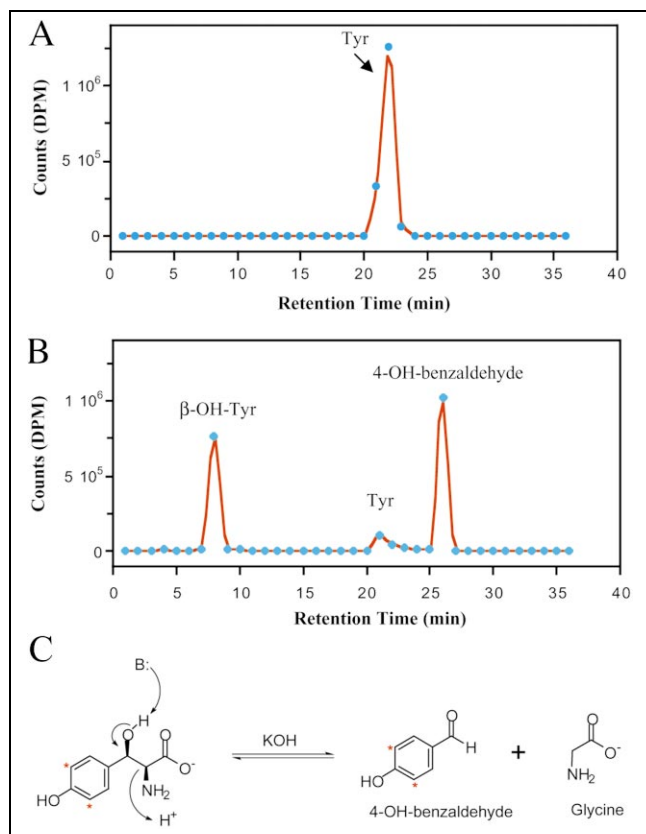


Fig. 7. HPLC separation and identification of [^3H]L-tyrosyl-S-NovH/NovI incubation products released by KOH treatment. At the end of incubation, the proteins were precipitated with 10% TCA and the protein pellets was washed with water to remove soluble small molecules. Then 0.1 M KOH was added to redissolve protein pellets and the resultant solution was incubated for 5 min at 60°C to hydrolyze the aminoacyl thioester linkage to NovH. Fractions (1 ml) from the RP-HPLC separation were collected and the radioactivity was measured by liquid scintillation counting. See Section 5 for detailed conditions. (A) Plot of radioactivity of the fractions versus rt (or fraction number) from the RP-HPLC analysis of the control reaction in which NovI was withdrawn. The released radioactive compound (rt=21.3 min) was proven to be [^3H]Tyr by co-injection. (B) Plot of radioactivity of fractions versus rt from the RP-HPLC analysis of the complete reaction. While there still remained a small [^3H]Tyr peak, the first new radioactive peak (rt=7.2 min) co-eluted with β -OH-Tyr and the second new radioactive peak had the same rt as 4-OH-benzaldehyde. (C) Schematic illustration of 4-OH-benzaldehyde formation from hydroxylated product β -OH-Tyr via a retro aldol reaction promoted by KOH. Since the tritium label is on the phenyl ring of the substrate L-Tyr, the breakdown product 4-OH-benzaldehyde is radioactive.

a cytochrome P450 monooxygenase that hydroxylates the β -carbon of the tethered L-tyrosyl group on NovH. The native electron donating proteins of *S. spheroides* are yet to be cloned, so commercially available spinach ferredoxin and ferredoxin reductase were used in the NovI incubations. In the incubation shown in Fig. 7B, a ratio of 4:1 for NovH:NovI was used and the incubation proceeded for 2 h at 24°C. No radioactive species other than starting [^3H]L-Tyr was detected in solution. To evaluate any product covalently bound to NovH, compounds were released

from NovH by KOH treatment to hydrolyze the aminoacyl-S-PCP thioester linkage and analyzed by reverse-phase high performance liquid chromatography (RP-HPLC) and scintillation counting. The radioactivity of fractions (1 ml in size) was plotted versus retention time (rt) to give Fig. 7B, while Fig. 7A shows the analysis of the identical reaction carried out in the absence of NovI. The released radioactive compound (rt=21.5 min) from the control reaction (Fig. 7A) was identified to be [^3H]L-Tyr, as established by co-injection (data not shown). In the reaction containing NovI, a much smaller substrate L-Tyr peak (rt=21.5 min) was presented, however, two new peaks with rts of 7.8 and 25.8 min were observed (Fig. 7B). The identity of first radioactive peak (rt=7.8 min) was initially established as L- β -OH-Tyr by co-elution with unlabeled authentic β -OH-Tyr added as carrier and monitored by UV (at 230 nm). In addition to the 7.8 min β -OH-Tyr peak, the HPLC UV chromatogram also detected another product peak that co-eluted with the 25.8 min radioactive peak, indicating this UV-active peak was likely derived from the added non-labeled carrier β -OH-Tyr. The KOH treatment during chemical release of the covalently tethered compound could promote a retro aldol reaction breaking down β -OH-Tyr to 4-OH-benzaldehyde, a process illustrated in Fig. 7C. Since the tritium label is at positions 3 and 5 of the phenyl ring of the input substrate [^3H]L-Tyr, the β -OH-Tyr breakdown product 4-OH-benzaldehyde will be tritiated. Co-injection of the incubation products with authentic 4-OH-benzaldehyde (Sigma) confirmed the comigration of the 25.8 min radioactive peak (data not shown).

A large-scale incubation with 60 nmol of NovH allowed isolation of enough products for mass characterization. The two product peaks were collected following RP-HPLC separation, lyophilized and subjected to matrix-assisted laser desorption ionization time-of-flight mass spectroscopy (MALDI-TOF MS) analysis. The measured masses of 198.1 and 122.1 ($\text{M}+\text{H}^+$ mode) matched well with the predicted values of β -OH-Tyr ($\text{C}_9\text{H}_{11}\text{NO}_4$, calc. 197.1) and 4-OH-benzaldehyde ($\text{C}_7\text{H}_6\text{O}_2$, calc. 122.0).

2.3.2. Properties of the NovI mediated hydroxylation reaction

To see if product formation catalyzed by NovI is proportional to the amount of substrate used, a series of incubations with varying amounts of [^3H]L-tyrosyl-S-NovH were performed and analyzed. A linear correlation of the amounts of product (β -OH-Tyr plus the breakdown product 4-OH-benzaldehyde) and the substrate protein NovH was observed (Fig. 8A).

As shown in Fig. 8B, when the amount of NovH was fixed at 3.1 nmol, and NovI was titrated down from 240 to 12 pmol, multiple turnovers on NovI were observed. At the 12 pmol lower limit, NovI displayed up to 55 turnovers towards its partner substrate protein L-Tyr-S-NovH. This result clearly demonstrates that NovH and NovI re-

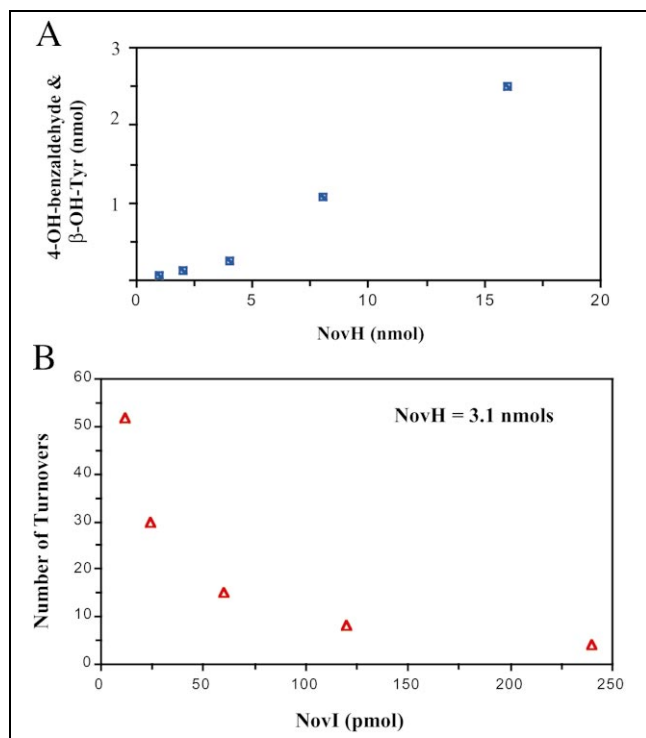


Fig. 8. (A) Total product formation ($[^3\text{H}]\beta\text{-OH-Tyr}$ plus $[^3\text{H}]4\text{-OH-benzaldehyde}$) was proportional to the amount of NovH used. (B) NovI functioned catalytically in the reaction and up to 55 turnovers were observed under the conditions described in Section 5.

constitute a competent enzymatic system for $\beta\text{-OH-tyrosyl-S-NovH}$ formation.

2.3.3. Determination of the stereochemistry of the new chiral center at the β -carbon of the tyrosyl moiety of *L-Tyr-S-NovH*

Although the newly generated chiral center of $\beta\text{-OH-}$

Tyr is lost at a later stage in coumarin biosynthesis (Fig. 1), it is still of interest to examine if the hydroxylation reaction effected by NovI is stereospecific and to establish the absolute stereochemistry. As shown in Fig. 9, the RP-HPLC-purified NovI product, $[^3\text{H}]\beta\text{-OH-Tyr}$, had the same rt (18.4 min) as chemically prepared (2*S*,3*R*)- $\beta\text{-OH-Tyr}$ (Fig. 9, trace C versus trace A) when analyzed by chiral HPLC (Daicel ChiralPAK WH[®]) [24,25]. Under the operating conditions, the (2*R*,3*S*) isomer (rt = 9.8 min) was well resolved from the (2*S*,3*R*) isomer (Fig. 9, trace B). Chiral HPLC analysis clearly indicated that the newly generated chiral center is an *R* center and that NovI makes a (2*S*,3*R*)-3-OH-Tyr-*S*-NovH covalent acyl enzyme.

3. Discussion

The results reported in this work establish enzymatic activities for the two proteins NovH and NovI from the novobiocin biosynthetic cluster and showed that amino-acylated NovH is a hydroxylation substrate for NovI. The bioinformatic-based predictions of an A and PCP domain in NovH [16] were validated with the purified enzyme. The A domain is specific for *L*-tyrosine, as assessed by an amino acid-dependent ATP- $[^{32}\text{P}]\text{PPi}$ exchange assay which monitors reversible formation of tyrosyl-AMP. The apo-PCP domain of NovH must be primed by covalent posttranslational phosphopantetheinylation. A dedicated PPTase for the *nov* cluster has not yet been identified so we used the broad specificity PPTase Sfp from the surfactin synthetase cluster of *Bacillus* [21]. The capture of the *L*-tyrosyl-AMP by the holo HS-pant-PCP domain of NovH was established by SDS-PAGE and trichloroacetic acid (TCA) precipitation assay with $[^3\text{H}]\text{L-tyr-}$

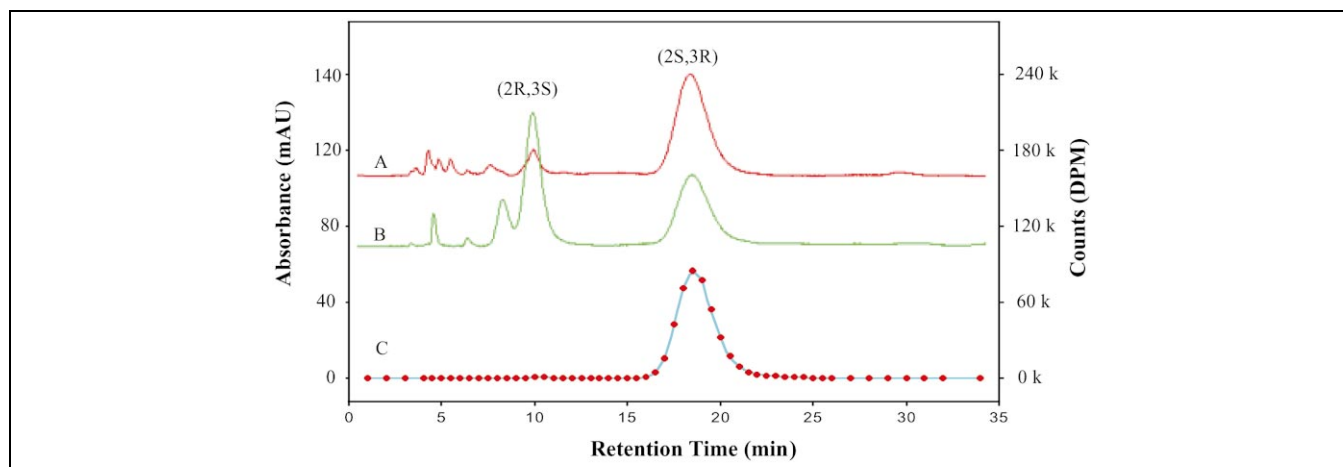


Fig. 9. Determination of the stereochemistry of the new chiral center in $\beta\text{-OH-tyrosyl}$ moiety introduced by NovI by chiral HPLC with ChiralPAK WH[®] from Daicel. Isocratic elution with 2.5 mM CuSO_4 at 1 ml/min was used and the UV detector was set at 272 nm. Trace A, HPLC chromatogram of chemically prepared authentic (2*S*,3*R*)- $\beta\text{-OH-Tyr}$ [24]. Trace B, HPLC chromatogram of chemically prepared racemic *threo* isomers, (2*S*,3*R*) and (2*R*,3*S*) $\beta\text{-OH-Tyr}$ [29]. The left Y-axis in mAU is for trace A and B. Trace C: plot of radioactivity of fractions (0.5 ml in size) versus rt from the analysis of the enzymatic product $[^3\text{H}]\beta\text{-OH-Tyr}$ by chiral HPLC. $[^3\text{H}]\beta\text{-OH-Tyr}$ was excised from NovH and isolated from RP-HPLC by collecting the 7.8 min peak (Fig. 7B). The right Y-axis in dpm is for plot C.

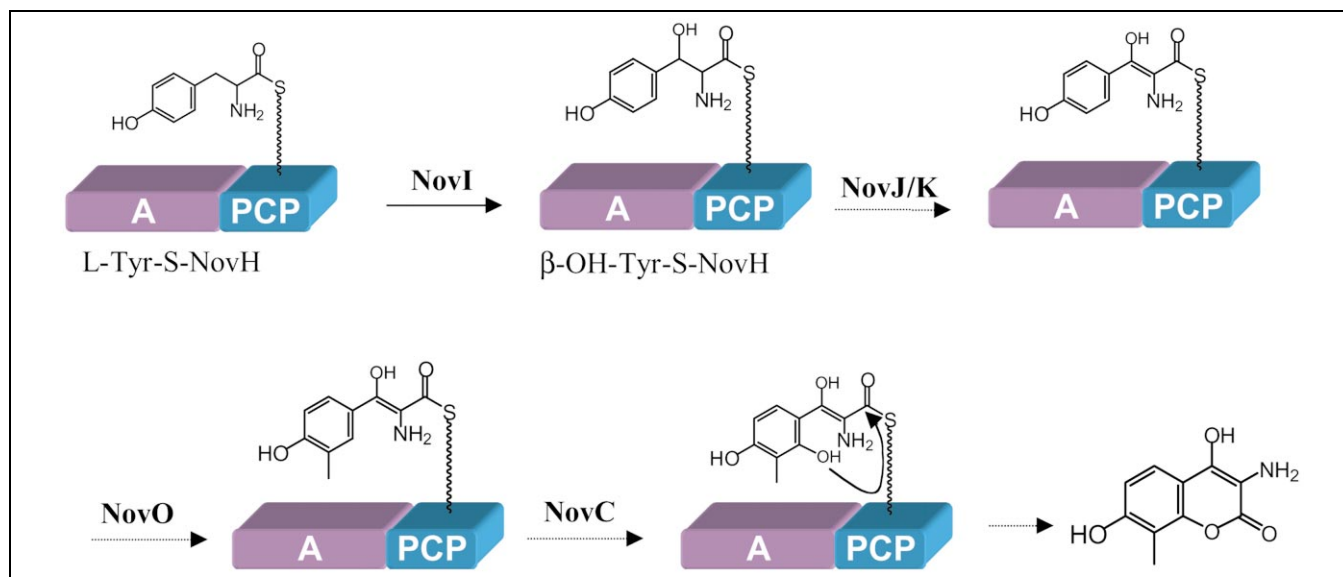


Fig. 10. Schematic illustration of the proposed pathway of aminocoumarin formation in the biogenesis of novobiocin. The functions of NovH and NovI have been established in this study. Both NovJ and NovK are similar to 3-keto-ACP reductase and they may form a heterodimer and operate in the reverse direction to oxidize 3-OH to 3-keto. NovO is similar to some quinone C-methyltransferases [30,31] but the timing of methylation is not clear. NovC resembles flavin-dependent monooxygenases (35 and 32% similarity to dimethylaniline and cyclohexanone monooxygenases, respectively) [32,33], and is proposed to hydroxylate the *ortho* position of the phenyl ring. The nucleophilic attack of the *ortho* hydroxyl group on the thioester carbonyl center would release the coumarin ring and regenerate NovH.

rosine to detect and quantitate the mole fraction of NovH accumulating as L-tyrosyl-S-NovH.

When the proposed companion protein NovI was purified it was red and contained one equivalent of heme co-factor. When provided with a heterologous electron donor system, spinach ferredoxin reductase and ferredoxin (the *S. sphaeroides* electron transfer proteins are yet to be cloned), to transfer electrons from NADPH, NovI utilized O_2 and performed as a catalytic monooxygenase. Initial assays indicated that NovI would not oxygenate free tyrosine or the soluble thioester surrogate L-tyrosyl-S-N-acetyl cysteamine (data not shown). Thus, NovI recognizes the L-tyrosyl moiety presented on the pantetheinyl arm of the PCP domain of NovH. NovI acts catalytically on its tyrosyl-S-NovH partner but the β-OH-Tyr product stays covalently tethered on the NovH PCP domain. To identify the β-OH-α-amino acid product, KOH was added to cleave the thioester linkage and thus allowed determination of the identity and stereochemistry of the β-hydroxylation product.

The question arises why NovI is specific for hydroxylation of the benzylic carbon of tyrosine tethered as a thioester on a partner protein. One answer comes from inspection of the structure of the coumarin ring B moiety of novobiocin. The coumarin is a two-ring lactone and the mechanism of lactonization has been inferred by ^{18}O labeling studies to be attack of the carboxyl oxygen on the aryl ring of Tyr in an oxidative cyclization [11]. However, ^{18}O enrichment of the ring oxygen was quite low (~ 0.078 at% excess) in that study and we favor a distinct pathway of lactonization, based on our enzymatic results and putative

functions of other ORFs in the *nov* cluster. Here we propose that the ring oxygen likely arises from hydroxylation by a predicted flavoprotein monooxygenase NovC (Fig. 10). Lactone formation would then arise by intramolecular capture of the proposed 2,4-dihydroxy-3-methyl-β-keto-Tyr-S-PCP of NovH as shown in Fig. 10. This is closely analogous to the intramolecular lactonizing step in 6-deoxyerythronolide biosynthesis [26] and in fengycin [27] biosynthesis by polyketide synthase (PKS) and NRPS assembly lines, respectively. The thermodynamic activation of the thioester moiety makes the cyclization and release from ACP/PCP carrier domains a favorable chain release step. The same logic applies for release of the coumarin from NovH.

This logic for coumarin ring assembly suggests the PCP domain of NovH is a scaffold on which the L-tyrosyl moiety is first covalently docked in kinetically stable but thermodynamically activated thioester linkage, and then chemically modified before cyclization. The pantetheinyl arm is 20 Å long if fully extended and this property may be crucial for providing access to the enzymes that will modify the tyrosyl backbone and ring. The first of these modifications is now proven to be the β-hydroxylation by NovI. Restriction of NovI activity to a tyrosine covalently tethered to the NovH PCP rather than free tyrosine may have advantages to the antibiotic-producing cell. It would control the fraction of the cellular pool of tyrosine that is hydroxylated and diverted to novobiocin formation. The companion ORFs to NovH and NovI include NovJ and NovK, predicted β-ketoacyl-carrier protein reductases [13], NovC, the proposed aromatic ring hydroxylating fla-

voprotein, and NovO, a predicted SAM-dependent C-methyltransferase [13]. The action of these three enzymes on β -OH-Tyr-*S*-NovH, as suggested in Fig. 10, would produce the 2,4-dihydroxy-3-methyl- β -keto-tyrosyl-*S*-NovH acyl-*S*-enzyme. Its intramolecular cyclizative capture would regenerate free NovH and yield the released lactone that is the coumarin ring found as the scaffold in the coumarin group antibiotics. NovJ could act alone to oxidize the β -hydroxyl group, but it is also possible that NovJ and NovK are subunits of single dimeric enzyme or represent two different isoenzymes. A comparable pair BbsC/BbsD, similar to 3-hydroxyacyl-CoA dehydrogenases, has been implicated in the β -oxidation of benzylsuccinate [28]. The timing of NovC and NovO action is as yet unknown, but our result that 3-methyl-L-Tyr was a very poor substrate for NovH (Table 1) argues that NovO acts downstream of NovH and NovI. The proposed pathway here would represent a novel use of the NRPS-type aminoacyl covalent tethering strategy and suggests that four tailoring enzymes, NovI, J/K, C and O, carry out sequential modification of a tyrosyl-*S*-pantetheinyl acyl enzyme.

In terms of maximizing metabolic economy it is possible that the β -OH-Tyr-*S*-NovH is also the source of the ring A 4-OH-benzoyl moiety of novobiocin. With the enzymically generated β -OH-Tyr and also with authentic samples we have seen facile retro aldol fragmentation across the C2–C3 bond to produce 4-OH-benzaldehyde and glycine. Oxidation of this aldehyde to the acid, perhaps after prenylation, could be effected by an oxidase to provide the ring A fragment of novobiocin.

Finally, a data base search for pairs of ORFs homologous to NovH and NovI that are found clustered together, reveals two other candidates, besides the pair in coumermycin A₁ CumC/CumD [18], that could analogously be activating amino acids as P-pant thioesters and then carrying out β -hydroxylation. One pair is ORF19 and ORF20 in the chloroeremomycin biosynthetic cluster [19], which is predicted to be a comparable A–PCP/P450 pair and this glycopeptide antibiotic of the vancomycin family indeed has a heptapeptide scaffold with (3*R*)- β -OH-Tyr residues at positions 2 and 6 [19]. In the biosynthetic cluster for the nucleoside antibiotic nikkomycin there is a corresponding A–PCP/P450 pair predicted, NikP1/NikQ, and we would assign NikQ as likely to be a monooxygenase producing a β -OH-His-*S*-PCP acyl-*S*-enzyme intermediate. It will be of interest to validate these predictions and see if NovI, CumD, ORF20 and NikQ do indeed form a new subgroup of cytochrome p450 monooxygenases committed to β -hydroxy amino acid formation on a segregated amino acid pool tethered to the PCP domains of partner proteins.

4. Significance

The antibacterial agents novobiocin, clorobiocin and coumermycin A₁ all contain a 3-amino-4-hydroxy-cou-

marin moiety that is a central scaffold for presentation of these antibiotics to their target, the N-terminal portion of the GyrB subunit of DNA gyrase. The biosynthesis of the bicyclic coumarin platform has been known to occur from tyrosine and presumably proceed through a β -OH-Tyr intermediate. The recent sequencing of the biosynthetic gene cluster for both novobiocin, and more recently, coumermycin A₁, has suggested that two proteins, NovH and NovI, would start the coumarin pathway and represent the first committed steps to tyrosyl β -hydroxylation. This work validates that the tyrosine molecules for coumarin ring formation are activated and tethered as covalent tyrosyl-*S*-NovH acyl enzyme species on the PCP domain of NovH, and that this tyrosine pool is the specific substrate for the partner enzyme NovI, a cytochrome P450 monooxygenase. The β -OH-Tyr-*S*-NovH product from NovI action is proposed to be a substrate for oxidation, cyclization and concomitant release of the 3-amino-4-hydroxy-coumarin from the NovH PCP domain. Homologs of the NovH/NovI pairs, found in other microorganisms that produce antibiotics containing β -hydroxyl amino acid moieties, such as the vancomycins and nikkomycins, suggest the hydroxylation of a tethered aminoacyl-*S*-PCP may be a general strategy for diversion of a fraction of the amino acid pool to modifications that provide building blocks for antibiotic biosynthesis.

5. Materials and methods

5.1. Cloning of *novH* and *novI* genes

The *novH* and *novI* genes of the novobiocin cluster were amplified from *S. spheroides* (ATCC26935) genomic DNA by polymerase chain reaction. Primers NovH-NtermNdeI (5'-GGA AGG CAT ATG TTC AAC ACT CGT GCG AAC AA-3') and NovH-CtermXhoI (5'-GCC TTC CTC GAG CTC CTC CAG GGT CGC TAT-3') were used to amplify the *novH* gene. The *novI* gene was amplified with primers NovI-NtermNdeI (5'-CCG ATA CAT ATG AGC ACC CGT CCG ACC GTG-3') and NovI-NtermXhoI (5'-GGG TAA CTC GAG GCC CGT GAT CCT GAT CGG-3'). The introduced NdeI and XhoI restriction sites of each primer are highlighted with boldface type. The amplified products were gel-purified, digested with NdeI and XhoI restriction enzymes, and ligated into pET24b and pET16b to give NovH C-terminal His6-tagged and NovI N-terminal His10-tagged constructs, respectively. The resulting plasmids, pHC10 and pHC21, were transformed into *E. coli* BL21(DE3) for protein overexpression.

5.2. Overexpression and purification of NovH and NovI proteins

Cells harboring pHC10 plasmid were grown in LB medium supplemented with 40 μ g/ml kanamycin. The cells were grown at 37°C to an OD₆₀₀ of 0.6, cooled to 24°C, induced with 50 μ M of IPTG and allowed to grow for an additional 6 h at

24°C. Growth of pHC21/BL21(DE3) involved inoculating 1 l of LB medium containing 100 mg ampicillin, 50 mg FeCl₃ and 50 mg δ -aminolevulinic acid with 10 ml of overnight culture, and was continued for 3 days at 15°C without IPTG induction. The cells from each 6 \times 1 l culture were harvested by centrifugation (10 min at 6000 \times g) and resuspended in 70 ml of buffer A (20 mM Tris–Cl, 0.2 M NaCl, 5 mM imidazole, pH 8.0). Resuspended cells were broken by French Press (two passages at 15000 psi) and the cell debris was removed by centrifugation (30 min at 35000 \times g). The supernatant was incubated with 4 ml of superflow nickel resin (Qiagen) for 2 h at 4°C. The resin was then packed into a column, washed with 20 bed volumes of wash buffer (buffer A plus 20 mM imidazole), and the protein was eluted by a linear gradient of 20–150 mM imidazole. Fractions containing the protein (judged by SDS–PAGE) were pooled, dialyzed against buffer B (20 mM Tris–Cl, 50 mM NaCl, 1 mM dithiothreitol, 10% glycerol, pH 7.5), concentrated, flash frozen in liquid nitrogen and stored at –80°C. Concentrations of the purified NovH and NovI were measured spectrophotometrically at 280 nm using the calculated extinction coefficient of 0.031 and 0.061 $\mu\text{M}^{-1}\text{cm}^{-1}$ for NovH and NovI, respectively.

5.3. Posttranslational modification of the NovH PCP domain with Sfp

A TCA precipitation assay [22] was adopted to measure the time course and the stoichiometry of the apo to holo conversion of NovH using *B. subtilis* PPTase enzyme Sfp. Reactions (200 μl , in duplicate) contained 75 mM Tris–Cl (pH 7.5), 5 mM MgCl₂, 10 mM Tris-(2-carboxyethyl)phosphine (TCEP; Sigma), 50 μM [³H]CoA (74 Ci/mol, DuPont NEN), 3.7 μM NovH and 0.3 μM of Sfp. Samples of 15 μl were withdrawn at various time points, and quenched with 0.5 ml of 10% TCA. The precipitated protein was pelleted, washed with 10% TCA, redissolved in 0.5 ml of 88% formic acid, and counted for radioactivity. Percent modification of NovH was calculated from the specific activity of the [³H]CoA and the NovH concentration.

5.4. ATP–[³²P]PP_i exchange assay for A domain activity

Reactions (100 μl) containing 75 mM Tris–Cl (pH 7.5), 5 mM MgCl₂, 5 mM TCEP, 2 mM ATP, 1.5 mM of amino acid substrate, 4 μM of NovH, and 1 mM [³²P]pyrophosphate (3.6 Ci/mol, DuPont NEN) were carried out at 24°C. The reactions were initiated by the addition of NovH and allowed to proceed for 25 min (5 min for L-Tyr), and then quenched with charcoal suspensions (500 μl of 1.6% (w/v) activated charcoal, 4.5% (w/v) tetrasodium pyrophosphate, and 3.5% perchloric acid in water). The charcoal was pelleted by centrifugation, washed twice with quenching buffer without added charcoal, and then resuspended in 0.8 ml of water and submitted for liquid scintillation counting. The amount of bound radioactivity was converted to reaction rate using the specific radioactivity of the [³²P]pyrophosphate. To determine kinetic parameters of L-Tyr, reactions were carried out at 24°C in a total volume of 100 μl that contained 75 mM Tris–Cl (pH 7.5), 5 mM MgCl₂, 5 mM TCEP, 2 mM ATP, 4 μM

NovH and 1 mM [³²P]pyrophosphate, and various amounts of L-Tyr. The reactions were terminated after 8 min incubation. For incubations of L-Phe, 3-Cl-L-Tyr, *p*-Br-DL-Phe, and 3-Me-L-Tyr, 12 μM of NovH was used and the reactions were allowed to continue for 23 min at 24°C.

5.5. Covalent aminoacylation of L-Tyr on the PCP domain of NovH

5.5.1. Autoradiography demonstrating auto-aminoacylation of [³H]L-Tyr to NovH

NovH was first primed with Sfp to install the P-pant group on the PCP domain. The incubation mixture (50 μl) included 75 mM Tris–Cl (pH 7.5), 5 mM MgCl₂, 0.1 mM [³H]Tyr (1 Ci/mmol, Dupont NEN), 5 mM TCEP, 2 mM ATP and 50 μM of NovH. The reaction was allowed to proceed for 30 min at 24°C and 8 μl was used for electrophoreses on 10% SDS–PAGE. Control reactions were carried out in parallel in which either the ATP was omitted or NovH was used without Sfp treatment. For visualization, the gel was stained with Coomassie brilliant blue solution, destained and soaked in Amplify (Amersham) for 15 min. The dried gel was exposed to film for 24 h before developing.

5.5.2. TCA precipitation assay

TCA precipitation assays were performed to measure the time course and the stoichiometry of auto-aminoacylation of L-Tyr by NovH. Reactions of 100 μl in volume contained 75 mM Tris–Cl (pH 7.5), 5 mM MgCl₂, 5 mM TCEP, 0.5 mM CoA, 0.2 μM Sfp, 10 μM NovH, 0.5 mM [³H]L-Tyr (90 Ci/mol) and 3 mM ATP, and incubated for 30 min at 24°C to allow the phosphopantetheinylation prior to initiation by the addition of ATP. Aliquots of 10 μl were withdrawn at various time points, quenched with 0.5 ml of 10% TCA, and the precipitated protein was pelleted, washed and counted for radioactivity. Percent auto-aminoacylation was calculated from the specific activity of the [³H]L-Tyr and the NovH concentration.

5.6. Incubation of NovI with L-tyrosyl-S-NovH

Holo NovH was loaded with [³H]L-Tyr at 24°C for 1.5 h in a reaction mixture (200 μl) that contained 75 mM Tris–Cl (pH 7.5), 5 mM MgCl₂, 0.5 mM [³H]L-Tyr (90 Ci/mol), 3 mM ATP, 2 mM TCEP and 40 μM NovH. Then NADPH, spinach ferredoxin (Sigma), ferredoxin reductase (Sigma), and NovI were added to a final concentration of 1.5 mM, 5 μM , 0.1 U and 10 μM , respectively. Incubation was allowed to continue for 2 h at 24°C prior to quenching with 1 ml of 10% TCA. The precipitated proteins were pelleted by centrifugation, washed three times with 1 ml water, and redissolved in 100 μl of 0.1 N KOH solution. The tethered product was released from the carrier protein by incubating for 5 min at 60°C. Routinely, a small amount of authentic non-labeled (2*S*,3*R*)- β -OH-Tyr (a gift from Dr. Manjinder S. Lall and Dr. Dale L. Boger of the Scripps Research Institute) [24] was added during the work-up as a non-labeled carrier compound. The proteins were removed by acidifying the mixture with 5 μl of 50% TFA followed by centrifugation. Prod-

uct formation was analyzed by HPLC using a Vydac[®] C18 small pore analytical column (5 μ m, 4.6 \times 250 mm) at 1 ml/min flow rate with monitor setting at 230 nm. The elution profile started with 100% solvent A (A = H₂O, 0.1% TFA) for 10 min, followed by a linear gradient from 0 to 50% solvent B (B = acetonitrile, 0.1% TFA) over 15 min. The radioactivity of fractions (1 ml) was measured by liquid scintillation counting of the collected samples. Plots of radioactivity versus fraction number were used to determine the *rt* of the product. A control incubation was carried out in parallel under the same conditions except that NovI was omitted.

5.7. Mass analyses of the NovI reaction products released from NovH

A large-scale incubation (2 ml) contained 75 mM Tris-Cl (pH 7.5), 50 mM NaCl, 5 mM MgCl₂, 3 mM ATP, 5 mM TCEP, 1.5 mM NADPH, 1 mM L-Tyr, 40 μ M of holo NovH, 5 μ M NovI, 5 μ M ferredoxin and 0.4 U ferredoxin reductase. Incubation proceeded for 1 h at 24°C for aminoacylation of NovH with L-Tyr prior to the addition of NovI, NADPH and the electron transfer proteins to initiate hydroxylation. The work up procedure noted above for radioactive incubations was followed. Two peaks that possessed the same *rt* as the (2*S*,3*R*)- β -OH-Tyr and 4-OH-benzaldehyde (Sigma) standards were collected from RP-HPLC, lyophilized and subjected to MALDI-TOF MS analysis.

5.8. Properties of the NovI mediated hydroxylation reaction

To examine whether NovI catalyzed product formation in a substrate-dependent fashion, a series of incubations (200 μ l) were carried out. Incubation mixtures contained 75 mM Tris-Cl (pH 7.5), 5 mM MgCl₂, 0.5 mM [³H]L-Tyr (90 Ci/mol), 2 mM ATP, 2 mM TCEP, 1 mM NADPH, 5 μ M ferredoxin, 0.1 U ferredoxin reductase, 10 μ M NovI, and various concentrations (5–80 μ M) of the holo NovH. After covalent loading of L-Tyr achieved by incubating at 24°C for 1.5 h, NovI and other necessary components were added to initiate the β -hydroxylation reaction. Reactions were terminated after 2 h at 24°C with 10% TCA. Work up and product analysis followed the procedure described above. In another experiment, catalytic amounts (ranging from 0.048 to 0.96 μ M in 250 μ l of reaction mixture) of NovI were used in the incubations while the concentration of NovH was kept at 12.4 μ M. Reactions were worked up and analyzed after 4 h incubation at 24°C.

5.9. Determination of the chirality of the β -OH center introduced by NovI

An incubation was carried out to prepare [³H] β -OH-Tyr following procedures described above. The pure product was obtained by RP-HPLC separation followed by lyophilization. The stereochemistry of the β center was established by chiral HPLC analysis with a ChiralPAK WH[®] column (Daicel) compared with chemically prepared reference samples of (2*S*,3*R*)-3-OH-Tyr [24] and racemic *threo* isomers (2*S*,3*R*)- and (2*R*,3*S*)-3-OH-Tyr [29].

Isocratic elution at 1 ml/min flow rate of 2.5 mM CuSO₄ was used. Fractions (0.5 ml) were collected and measured for radioactivity by a liquid scintillation counter to determine the *rt* of the enzymatic product. When analyzing unlabeled reference compounds, their *rt*s were measured by monitoring at 272 nm with an UV-detector.

Acknowledgements

We thank Dr. Manjinder S. Lall and Dr. Dale L. Boger of the Scripps Research Institute for the generous gift of (2*S*,3*R*)-3-OH-tyrosine and Dr. Steven Rokita and Ms. Jessica Friedman of the University of Maryland for 3-methyl-L-tyrosine. We also thank Dr. Brian K. Hubbard for providing the racemic *threo* isomers of 3-OH-tyrosine, and Dr. Michael D. Burkart and Dr. John W. Trauger for L-tyrosyl-*S*-*N*-acetyl cysteamine. This work was supported by NIH Grant GM 20011.

References

- [1] H. Celia, L. Hoermann, P. Schultz, L. Lebeau, V. Mallouh, D.B. Wigley, J.C. Wang, C. Mioskowski, P. Oudet, Three-dimensional model of *Escherichia coli* gyrase B subunit crystallized in two-dimensions on novobiocin-linked phospholipid films, *J. Mol. Biol.* 236 (1994) 618–628.
- [2] A. Maxwell, The interaction between coumarin drugs and DNA gyrase, *Mol. Microbiol.* 9 (1993) 681–686.
- [3] A. Maxwell, DNA gyrase as a drug target, *Trends Microbiol.* 5 (1997) 102–109.
- [4] R.J. Lewis, O.M.P. Singh, C.V. Smith, T. Skarzynski, A. Maxwell, A.J. Wonacott, D.B. Wigley, The nature of inhibition of DNA gyrase by the coumarins and cyclothialidines revealed by X-ray crystallography, *EMBO J.* 15 (1996) 1412–1420.
- [5] L.L. Shen, Quinolone–DNA interaction, in: D.C. Hooper, J.S. Wolfson (Eds.), *Quinolone Antimicrobial Agents*, American Society for Microbiology, Washington, DC, 1993, pp. 77–95.
- [6] A. Sugino, N.P. Higgins, P.O. Brown, C.L. Peebles, N.R. Cozzarelli, Energy coupling in DNA gyrase and the mechanism of action of novobiocin, *Proc. Natl. Acad. Sci. USA* 75 (1978) 4838–4842.
- [7] F.T.F. Tsai, O.M. Singh, T. Skarzynski, A.J. Wonacott, S. Weston, A. Tucker, R.A. Pauptit, A.L. Breeze, J.P. Poyser, R. O'Brien, J.E. Ladbury, D.B. Wigley, The high-resolution crystal structure of a 24-kDa gyrase B fragment from *E. coli* complexed with one of the most potent coumarin inhibitors, clorobiocin, *Proteins* 28 (1997) 41–52.
- [8] D.C. Hooper, J.S. Wolfson, G.L. McHugh, M.B. Winters, M.N. Swartz, Effects of novobiocin, coumermycin A₁, clorobiocin, and their analogs on *Escherichia coli* DNA gyrase and bacterial growth, *Antimicrob. Agents Chemother.* 22 (1982) 662–671.
- [9] N.A. Gormley, G. Orphanides, A. Meyer, P.M. Cullis, A. Maxwell, The interactions of coumarin antibiotics with fragment of the DNA gyrase B protein, *Biochemistry* 35 (1996) 5083–5092.
- [10] A.J. Birch, P.W. Holloway, R.W. Richards, The biosynthesis of noviose, a branched-chain monosaccharide, *Biochim. Biophys. Acta* 57 (1962) 143–145.
- [11] C.A. Bunton, G.W. Kenner, J.T. Robinson, B.R. Webster, Experiments related to the biosynthesis of novobiocin and other coumarins, *Tetrahedron* 19 (1963) 1001–1010.
- [12] R.T. Calvert, M.S. Spring, J.R. Stoker, Investigations of the biosynthesis of novobiocin, *J. Pharm. Pharmacol.* 24 (1972) 972–978.

- [13] M. Steffensky, A. Muhlenweg, Z.X. Wang, S.M. Li, L. Heide, Identification of the novobiocin biosynthetic gene cluster of *Streptomyces spheroides* NCIB 11891, *Antimicrob. Agents Chemother.* 44 (2000) 1214–1222.
- [14] M. Steffensky, S.M. Li, L. Heide, Cloning, overexpression, and purification of novobiocin acid synthetase from *Streptomyces spheroides* NCIB 11891, *J. Biol. Chem.* 275 (2000) 21754–21760.
- [15] M.A. Marahiel, T. Stachelhaus, H.D. Mootz, Modular peptide synthetases involved in nonribosomal peptide synthesis, *Chem. Rev.* 97 (1997) 2651–2673.
- [16] T. Stachelhaus, H.D. Mootz, M.A. Marahiel, The specificity-conferring code of adenylation domains in nonribosomal peptide synthetases, *Chem. Biol.* 6 (1999) 493–505.
- [17] G.L. Challis, J. Ravel, C.A. Townsend, Predictive, structure-based model of amino acid recognition by nonribosomal peptide synthetase adenylation domains, *Chem. Biol.* 7 (2000) 211–244.
- [18] Z.X. Wang, S.M. Li, L. Heide, Identification of the coumermycin A₁ biosynthetic gene cluster of *Streptomyces rishiriensis* DSM 40489, *Antimicrob. Agents Chemother.* 44 (2000) 3040–3048.
- [19] A.M. van Wageningen, P.N. Kirkpatrick, D.H. Williams, B.R. Harris, J.K. Kershaw, N.J. Lennard, M. Jones, S.J. Jones, P.J. Solenberg, Sequencing and analysis of genes involved in the biosynthesis of a vancomycin group antibiotic, *Chem. Biol.* 5 (1998) 155–162.
- [20] B. Lauer, R. Russwurm, C. Bormann, Molecular characterization of two genes from *Streptomyces tendae* Tu901 required for the formation of the 4-formyl-4-imidazolin-2-one-containing nucleoside moiety of the peptidyl nucleoside antibiotic nikkomycin, *Eur. J. Biochem.* 267 (2000) 1698–1706.
- [21] L.E.N. Quadri, P.H. Weinreb, M. Lei, M.M. Nakano, P. Zuber, C.T. Walsh, Characterization of Sfp, a *Bacillus subtilis* phosphopantetheinyl transferase for peptidyl carrier protein domains in peptide synthetases, *Biochemistry* 37 (1998) 1585–1595.
- [22] R.H. Lambalot, A.M. Gehring, R.S. Flugel, P. Zuber, M. LaCelle, M.A. Marahiel, R. Reid, C. Khosla, C.T. Walsh, A new enzyme superfamily: the phosphopantetheinyl transferases, *Chem. Biol.* 3 (1996) 923–936.
- [23] T.A. Keating, D.A. Miller, C.T. Walsh, Expression, purification, and characterization of HMWP2, a 229 kDa, six domain protein subunit of yersiniabactin synthetase, *Biochemistry* 39 (2000) 4729–4739.
- [24] D. Seebach, E. Juaristi, D.D. Miller, D. David, C. Schikli, T. Weber, Addition of chiral glycine, methionine, and vinylglycine enolate derivatives to aldehydes and ketones in the preparation of enantiomerically pure α -amino- β -hydroxy acids, *Helv. Chim. Acta* 70 (1987) 237.
- [25] R.B. Herbert, B. Wilkinson, G.J. Ellames, E.K. Kunec, Stereospecific lysis of a range of β -hydroxy- α -amino acids catalyzed by a novel aldolase from *Streptomyces amakusaensis*, *J. Chem. Soc. Chem. Commun.* (1993) 205–206.
- [26] R.S. Gokhale, D. Hunziker, D.E. Cane, C. Khosla, Mechanism and specificity of the terminal thioesterase domain from the erythromycin polyketide synthase, *Chem. Biol.* 6 (1999) 117–125.
- [27] S. Steller, D. Vollenbroich, F. Leenders, T. Stein, B. Conrad, J. Hofemeister, P. Jacques, P. Thonart, J. Vater, Structural and functional organization of the fengycin synthetase multienzyme system from *Bacillus subtilis* b213 and A1/3, *Chem. Biol.* 6 (1999) 31–41.
- [28] B. Leuthner, J. Heider, Anaerobic toluene catabolism of *Thauera aromatica*: the *bbs* operon codes for enzymes of β oxidation of the intermediate benzylsuccinate, *J. Bacteriol.* 182 (2000) 272–277.
- [29] W.A. Bolhofer, The preparation of hydroxyphenylserine from benzyl-oxybenzaldehydes and glycine, *J. Chem. Soc.* 76 (1954) 1322–1323.
- [30] R.J. Barkovich, A. Shtanko, J.A. Shepherd, P.T. Lee, D.C. Myles, A. Tzagoloff, C.F. Clarke, Characterization of the COQ5 gene from *Saccharomyces cerevisiae*. Evidence for a C-methyltransferase in ubiquinone biosynthesis, *J. Biol. Chem.* 272 (1997) 9128–9128.
- [31] P.T. Lee, A.Y. Hsu, H.T. Ha, C.F. Clarke, A C-methyltransferase involved in both ubiquinone and menaquinone biosynthesis: isolation and identification of the *Escherichia coli* ubiE gene, *J. Bacteriol.* 179 (1997) 1748–1754.
- [32] V. Khalameyzer, I. Fischer, U.T. Bornscheuer, J. Altenbuchner, Screening, nucleotide sequence, and biochemical characterization of an esterase from *Pseudomonas fluorescens* with high activity towards lactones, *Appl. Environ. Microbiol.* 65 (1999) 477–482.
- [33] E. Atta-Asafo-Adjei, M.P. Lawton, R.M. Philpot, Cloning, sequencing, distribution, and expression in *Escherichia coli* of flavin-containing monooxygenase 1C1. Evidence for a third gene subfamily in rabbits, *J. Biol. Chem.* 268 (1993) 9681–9689.